Title: The Val66Met Polymorphism Alters the BDNF Prodomain Structure to Induce Neuronal Growth Cone Retraction.

Authors: Agustin Anastasia[1], Katrin Deinhardt[2,5], Moses V. Chao[2], Nathan E. Will[1], Krithi Irmady[1], Francis S. Lee[3], Barbara L. Hempstead[1*], Clay Bracken[4*].

Supplementary Figure S1.

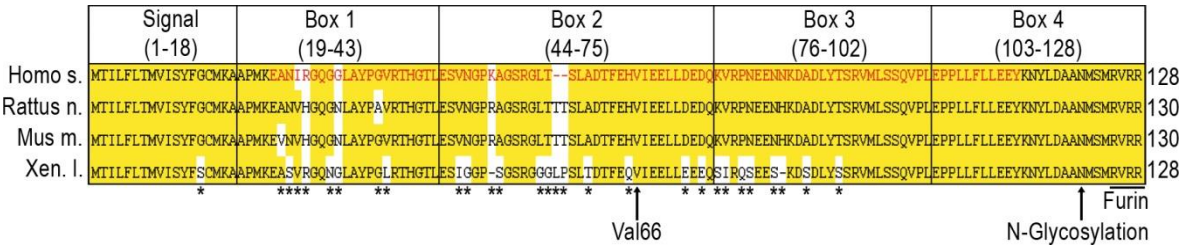

Supplementary Figure S1. **Sequence alignments of the BDNF prodomain from *Homo sapiens, Rattus norvegicus, Mus musculus* and *Xenopus laevis* show the high sequence conservation.** The recombinant protein produced for this study is highlighted in red. The signal peptide and four "boxes" are delineated based on amino acid conservation between BDNF, NGF and NT-3, as was labeled in a mutagenesis study of the NGF prodomain[17,49]. Val66Met polymorphism site and the N-glycosylation site are shown with arrows. Furin cleavage sequence is underlined. Alignments were performed with ClustalW2 software (http://www.ebi.ac.uk/Tools/msa/clustalw2/) and the asterisks represent the nucleotides not conserved between all the sequences.

Supplementary Figure S2.

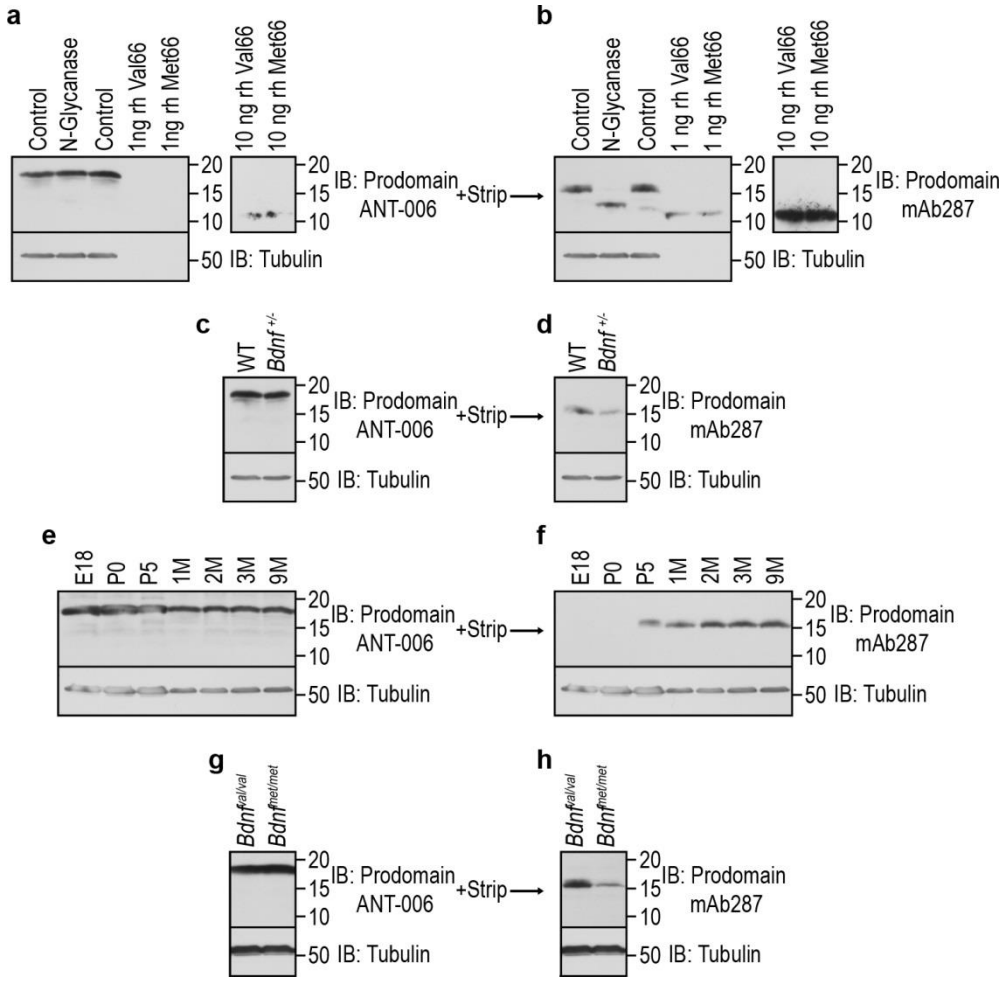

Supplementary Figure S2. The ANT-006 antibody to the prodomain of BDNF (Alomone, Jerusalem, Israel) failed to detect the endogenous prodomain in isolation and showed very low sensitivity detecting the recombinant prodomains. Hippocampal lysates and recombinant prodomains were resolved using SDS-PAGE, then transferred followed by membranes fixation with 2.5% glutaraldehyde (Sigma) in phosphate buffered saline pH 7.4. After blocking with 5% bovine serum albumin (BSA) in Tris-buffered saline with 0.1% Tween 20, membranes were incubated with BDNF prodomain antibody ANT-006 (1:1500, 12-16hs at 4C; panels a, c, e and g), followed by anti-rabbit horse radish peroxidase (HRP) secondary antibody (1:5000, 1h at 20-25C, Calbiochem-Millipore). After ECL detection of the bands, the membranes were stripped and incubated with BDNF

prodomain antibody mAb287 (1:2000, 12-16hs at 4C, GeneCopoeia; panels b, d, f, and h), followed by anti-mouse horse radish peroxidase (HRP) secondary antibody (1:5000, 1h at 20-25C, Calbiochem-Millipore). (a) ANT-006 antibody detected an 18 to19 kDa band in the hippocampal lysates that did not drop in molecular weight after treatment with N-glycanase, as compared to the 15.5 kDa band detected by the mAb287 antibody (b). Control = hippocampal lysate with deglycosylation buffer but without addition of N-glycanase. Moreover, the ANT-006 antibody was not sensitive enough to detect 1 nanogram (ng) of recombinant human (rh) Val66 or Met66 prodomains (a), as compared to the mAb287 antibody (b). The ANT-006 antibody was able to detect faintly 10 nanograms of recombinant prodomains (a), in contrast to the very sensitive mAb287 (b). (c) Using the ANT-006 antibody there was no decrease in the intensity of the 18-19 kDa band in the *Bdnf* heterozygote ($Bdnf^{+/-}$) hippocampal lysates, as compared to the decrease observed in the 15.5 kDa band in $Bdnf^{+/-}$ with the mAb287 antibody (d). (e) The ANT-006 antibody-positive 18-19 kDa band was detected in the hippocampal lysates of all the developmental time points studied. Instead, 15.5 kDa band detected with the mAb287 antibody (f) was developmentally regulated in agreement with previously published studies for mBDNF[10,30,31]. There was no change in the intensity of the 18-19 kDa band in hippocampal lysates with the ANT-006 antibody in the $Bdnf^{met/met}$ mice as compared to the $Bdnf^{val/val}$. However, the 15.5 kDa band detected with the mAb287 antibody showed a significant decrease consistent with a previous report which found decrease BDNF in these knock-in animals by enzyme-linked immunosorbent assay[32].

Supplementary Figure S3.

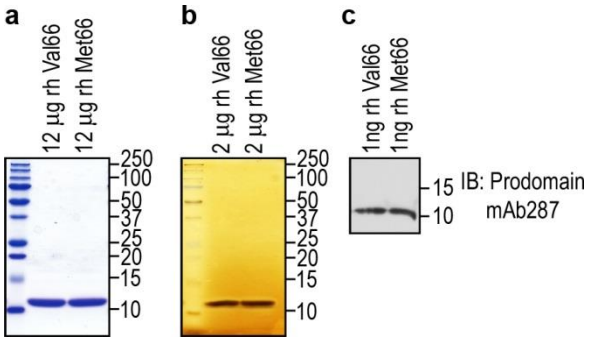

Supplementary Figure S3. Analysis of the recombinant Val66 and Met66 prodomains. Recombinant human (rh) Val66 or Met66 prodomains were subjected to SDS-PAGE and then visualized by staining of the gel with Coomassie blue (a) or silver staining (b). By both staining we found high purity that was estimated by densitometry analysis using Image J. (c) Detection of recombinant Val66 or Met66 using proBDNF antibodies (mAb287). There was no difference in the detection of the Val66 and Met66 prodomains by this specific prodomain antibody. In (a), (b), and (c) the prodomain runs at ~10.2 kDa which is the predicted molecular weight of the recombinant prodomain by its amino acid sequence.

Supplementary Figure S4

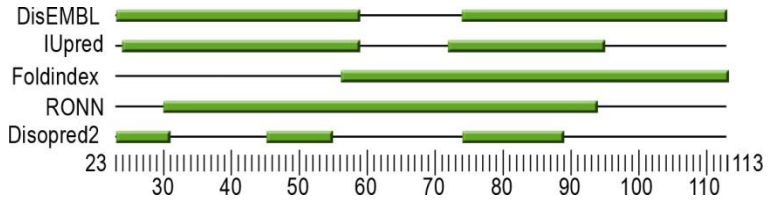

Supplementary Figure S4. Disorder prediction of the Val66 prodomain. The predictions were achieved using DisEMBL (http://dis.embl.de), IUpred (http://iupred.enzim.hu), Foldindex (http://bip.weizmann.ac.il/fldbin/findex), RONN (http://www.strubi.ox.ac.uk/RONN/) and Disopred2 (http://bioinf.cs.ucl.ac.uk/disopred/) software. Disordered regions in the amino acid sequence are displayed as green boxes, and the numbers represent the amino acid position within the BDNF prodomain.

Supplementary Figure S5.

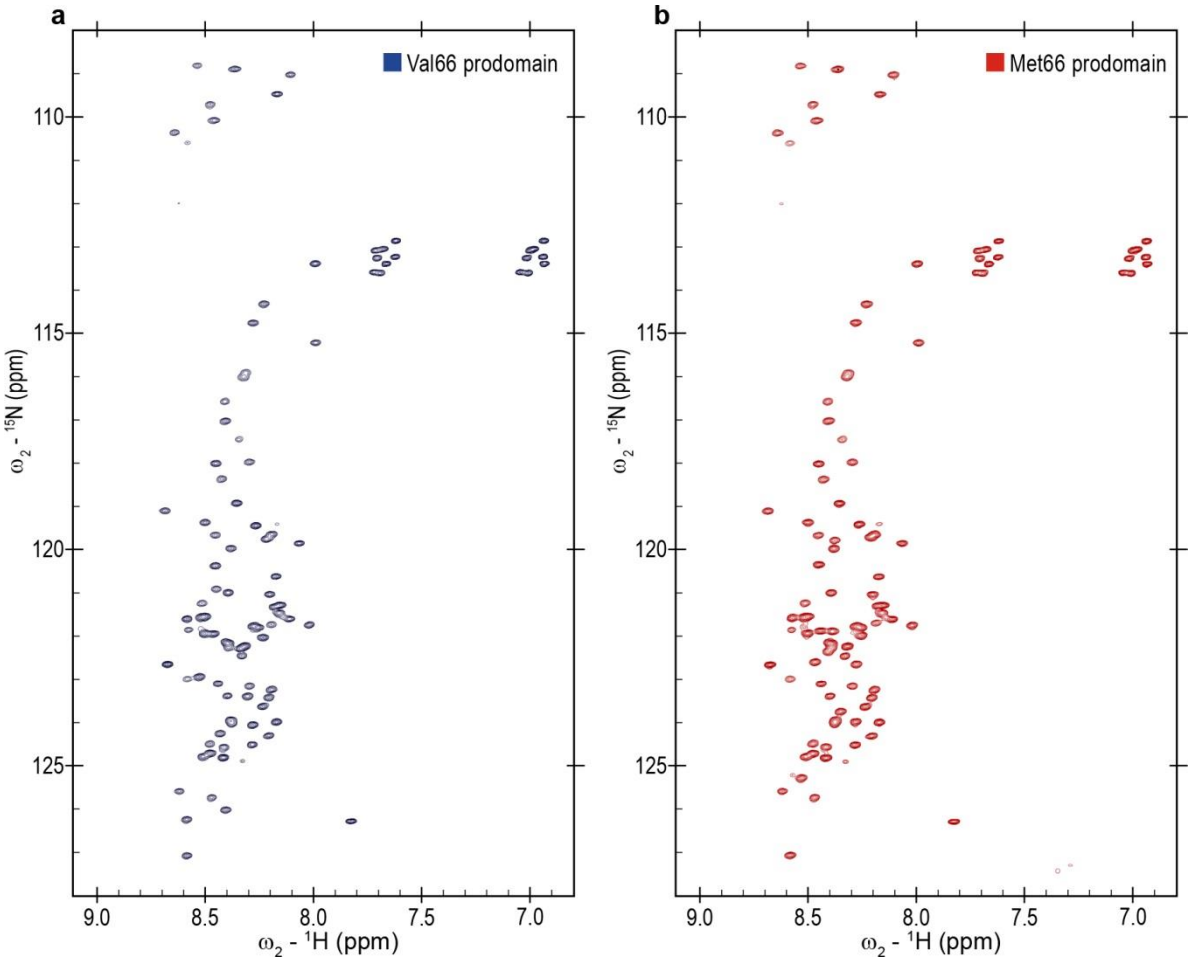

Supplementary Figure S5. Impact of the Val66Met substitution on the NMR spectrum of the BDNF prodomains. (a, b) Heteronuclear single-quantum coherence (HSQC) spectra. Each cross-peak (chemical shift) corresponds to one residue within the sequence of the prodomain (one chemical shift for each covalently bonded pair of ^{1}H-^{15}N atoms assigned to specific amides within the prodomain sequence). (a) ^{1}H-^{15}N-labeled Val66 prodomain HSQC spectra collected at 600 MHz (blue). (b) ^{1}H-^{15}N-labeled Met66 prodomain HSQC spectra collected at 600 MHz (red). Both protein spectra were collected in 50 mM NaH_2PO_4 100 mM NaCl, pH 7.0 buffer at 7ºC, at concentrations of ~20μM. The overlay of both HSQC spectra is shown in Fig. 3.

Supplementary Figure S6.

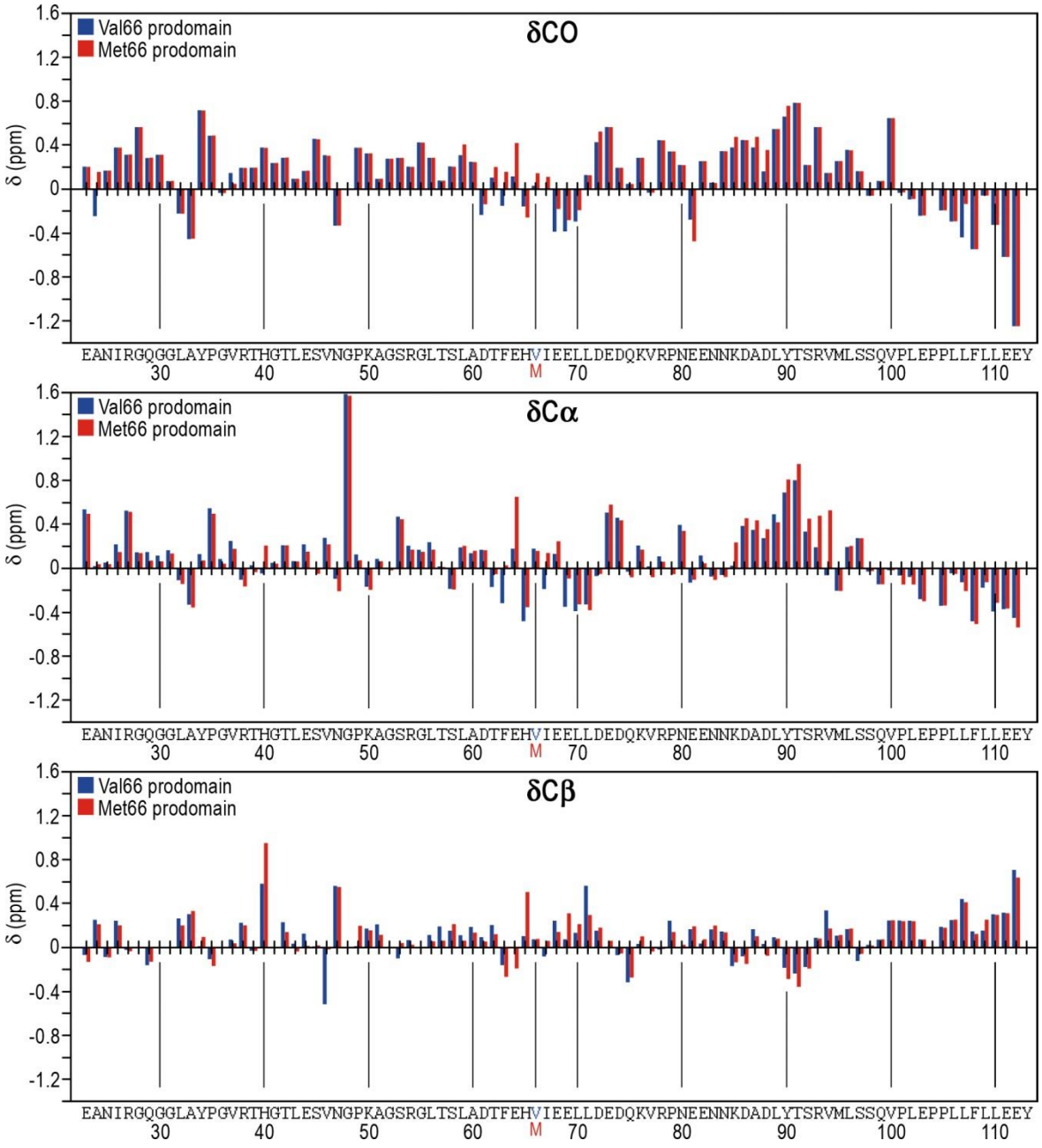

Supplementary Figure S6. Secondary chemical shifts analysis for the Val66 prodomain and the Met66 prodomain indicate that both are primarily disordered structures. The deviations of the Val66 prodomain (blue bars) and Met66 prodomain (red bars) chemical shifts were calculated from random-coil values[50]. The measured CO, CA and CB prodomain shifts were obtained from triple resonance HNCO, HNCA, and CBCA(CO)NH spectra.

Supplementary Figure S7.

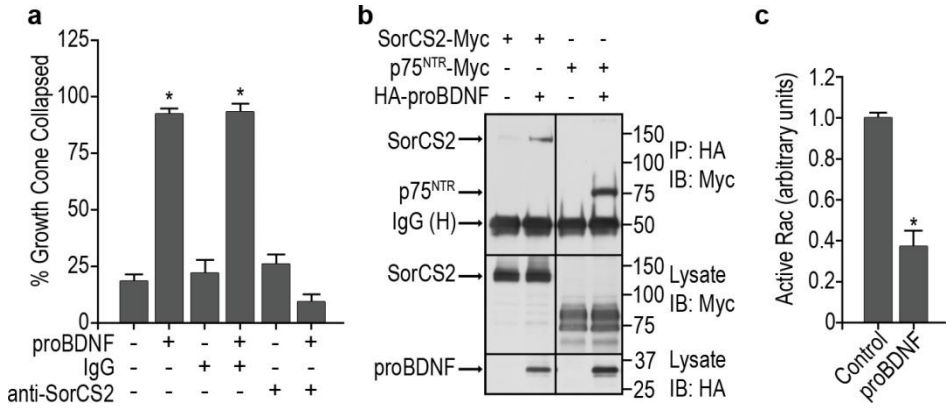

Supplementary Figure S7. proBDNF induces growth cone retraction in cultured hippocampal neurons. (a) Quantification of growth cone retraction in $p75^{NTR}$ positive cells after 20 minutes of treatment with proBDNF (10 ng/ml). Pre-incubated with anti-SorCS2 (or control IgGs) was able to block proBDNF-induced growth cone retraction. n=4 independent experiments. (b) HEK293T cells were transfected with the indicated constructs, the lysates were immunoprecipitated with anti-HA antibody, followed by detection with indicated antibodies. Representative blot of 3 independent experiments. (c) proBDNF induced a decrease in Rac activity in cultured hippocampal neurons. Activated Rac (Rac-GTP) was isolated with GST–PAK-CRIB beads and measured by densitometry and normalized to total Rac in the input. Quantification assessed in 4 independent experiments. Bars represent mean ± s.e.m. Statistical comparisons were made by one way analysis of variance test. * $p < 0.05$.

Supplementary Figure S8.

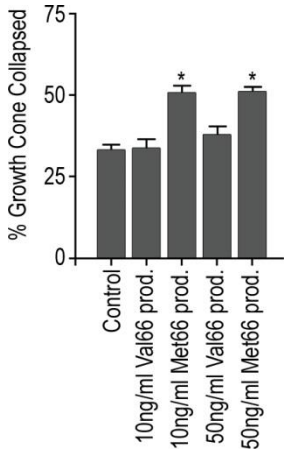

Supplementary Figure S8. Growth cone retraction assay in cultured hippocampal neurons. Neurons were treated with Val66 or Met66 prodomains (10 and 50 ng/ml) for 20 min followed by growth cone retraction analysis. Quantification assessed in $p75^{NTR}$ positive cells from 4 independent experiments. Bars represent mean ± s.e.m. Statistical comparisons were made by one way analysis of variance test. * $p < 0.05$.

Supplementary Figure S9.

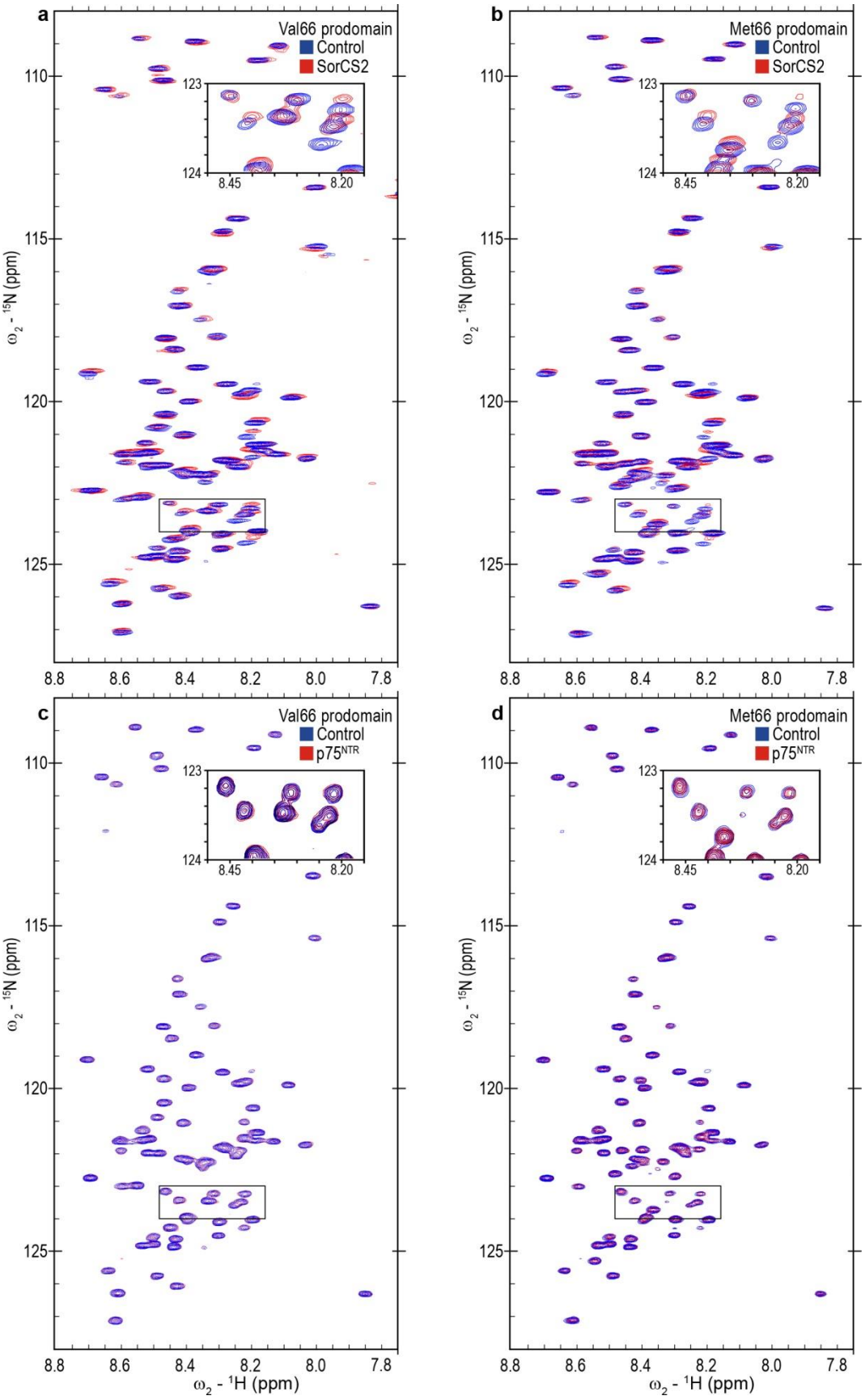

Supplementary Figure S9. NMR spectrum of the Val66 and Met66 prodomains with or without addition of SorCS2 or $p75^{NTR}$. (a) Heteronuclear single-quantum coherence (HSQC) spectra of the Val66 prodomain with or without SorCS2. (b) HSQC spectra of the Met66 prodomain with or without SorCS2. (c) HSQC spectra of the Val66 prodomain with or without $p75^{NTR}$. (d) HSQC spectra of the Met66 prodomain with or without $p75^{NTR}$. All spectra were collected at 4.4μM concentration of receptors and prodomains (1:1 ratio), in 50 mM NaH_2PO_4 100 mM NaCl, pH 6.8 buffer at 7ºC. Quantification of the chemical shift differences are shown in Fig. 6 d, e.

Supplementary Figure S10.

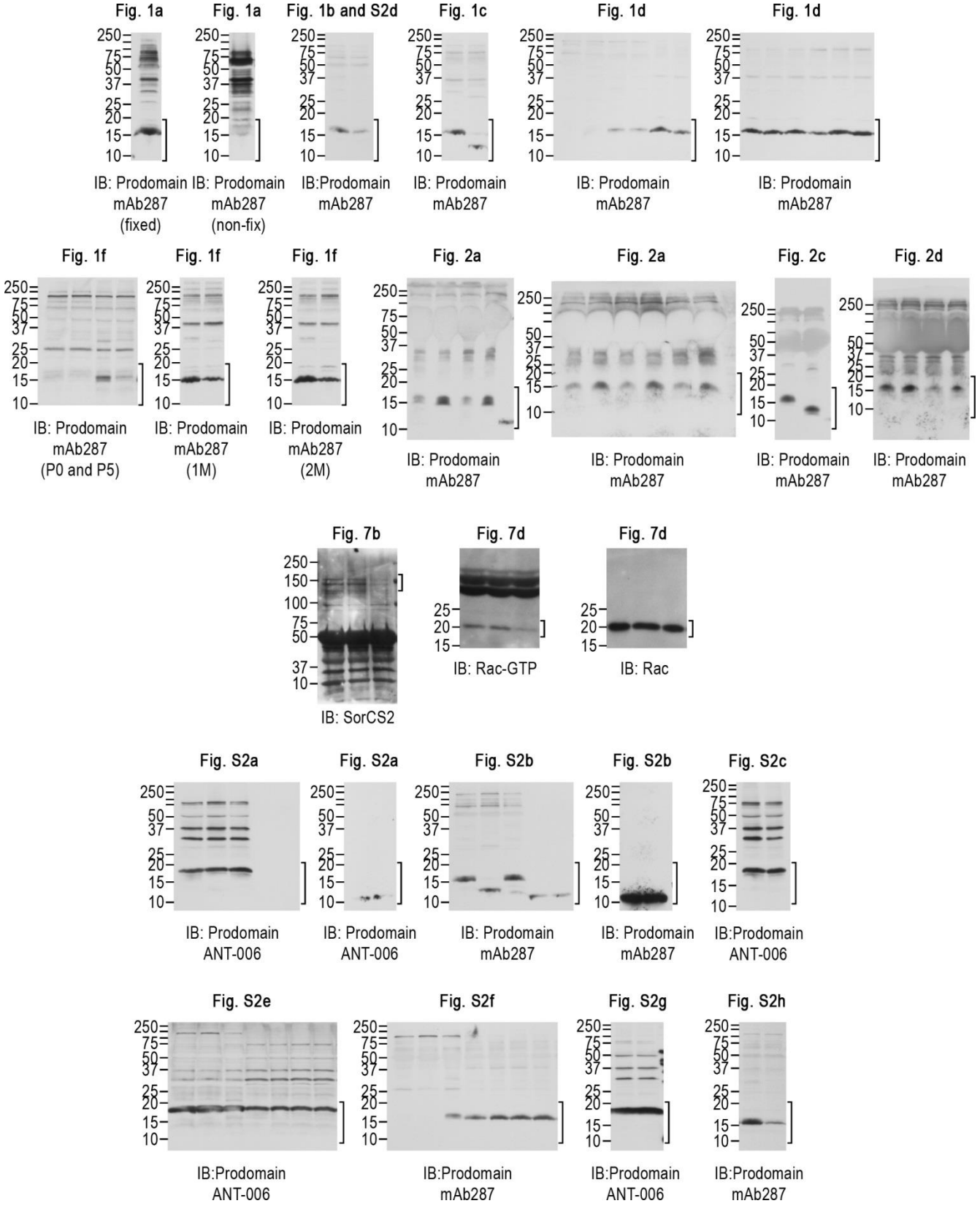

Supplementary Figure S10. Full gel scans.] = Region displayed in the main figures.

Supplementary Table S1. NMR diffusion measurements.

Sample	Measured[a] D_T (10^{-10} m^2 s^{-1})	R_h radii (A)[b]	hydrodynamic volume (nm^3)
Dioxane	10.8	2.12[a]	0.038
Lysozyme	1.30	17.6[c]	22.8
Val66 prodomain	1.02	22.4	47.4
Met66 prodomain	1.04	22.0	44.7
Val66 + SorCS2[d]	0.99	23.1	51.8
Met66 + SorCS2[d]	0.73	31.3	129.2

[a]The error in diffusion measurements is 5%.

[b]Dioxane is used as an internal diffusion reference[47], calculated hydrodynamic radii and molecular weights are shown.

[c]The non-hydrated radius of native 14.3 kDa hen lysozyme is calculated to be 16.0Å[51].

[d]The unlabeled SorCS2 NMR signals entirely decay due to spin relaxation during the BPP-LED pulse sequence and therefore do no contribute to measured prodomain peak intensity changes.

Supplementary References

49 Suter, U., Heymach, J. V., Jr. & Shooter, E. M. Two conserved domains in the NGF propeptide are necessary and sufficient for the biosynthesis of correctly processed and biologically active NGF. *Embo j* **10**, 2395-2400 (1991).

50 Tamiola, K., Acar, B. & Mulder, F. A. Sequence-specific random coil chemical shifts of intrinsically disordered proteins. *J Am.Chem.Soc.* **132**, 18000-18003 (2010).

51 Chou, J. J., Baber, J. L. & Bax, A. Characterization of phospholipid mixed micelles by translational diffusion. *Journal of biomolecular NMR* **29**, 299-308, doi:10.1023/B:JNMR.0000032560.43738.6a (2004).